The effect of magnesium added at C60/Rubrene heterointerfaces

Chiu-Ping Cheng, Cheng-Wei Lee, Yu-Ya Chu, Ching-Hsuan Wei, and Tun-Wen Pi

Citation: Journal of Applied Physics **114**, 243704 (2013); doi: 10.1063/1.4854815
View online: http://dx.doi.org/10.1063/1.4854815
View Table of Contents: http://scitation.aip.org/content/aip/journal/jap/114/24?ver=pdfcov
Published by the AIP Publishing

The effect of magnesium added at C_{60}/Rubrene heterointerfaces

Chiu-Ping Cheng (鄭秋平),[1,a)] Cheng-Wei Lee (李正偉),[1] Yu-Ya Chu (屈郁雅),[1] Ching-Hsuan Wei (魏竟軒),[2] and Tun-Wen Pi (皮敦文)[3]
[1]*Department of Electrophysics, National Chiayi University, Chiayi 60004, Taiwan*
[2]*Department of Material Science, National Chiao-Tung University, Hsinchu 30076, Taiwan*
[3]*National Synchrotron Radiation Research Center, Hsinchu 30076, Taiwan*

(Received 7 November 2013; accepted 9 December 2013; published online 26 December 2013)

This study examines the effect of adding magnesium (Mg) at C_{60}/rubrene heterointerfaces by using synchrotron-radiation photoemission spectroscopy. The heterointerface was obtained by depositing C_{60} on a 4-Å Mg/rubrene surface. The photoemission spectra showed that the added Mg preferentially interacts with and transfers negative charges to C_{60}. The interfacial dipole potential was significantly enlarged, as was the separation between the lowest unoccupied molecular orbital of C_{60} and the highest occupied molecular orbital of rubrene. The results demonstrate that the addition of Mg should be an effective method for improving the efficiency of light- and current-generating devices. © *2013 AIP Publishing LLC*. [http://dx.doi.org/10.1063/1.4854815]

Rubrene ($C_{42}H_{28}$, 5,6,11,12-tetraphenylnaphthacene) is a versatile molecular material suitable for organic electronics applications.[1–5] A recent unexpected finding was that the rubrene:C_{60} heterostructure could be used to produce an organic dual device (ODD), which successfully integrates light- and current-generation functions.[4] The solar power conversion efficiency of this device reaches 3%, not yet meeting commercial criteria. Doping is a simple approach to improving organic semiconductor devices, and multiple methods are available for increasing the efficiency of organic devices by incorporating atoms or molecules into them.[2,6,7] However, to find potential additives, the energy-level offsets at heterointerfaces incorporating the dopants must be understood; this is because of the fundamental nature of light- and current-generation processes in organic materials. Therefore, the electronic structures of the corresponding heterointerfaces must be studied.

In this study, magnesium (Mg) was added at the C_{60}/rubrene interface. The heterointerface was obtained by depositing C_{60} on a 4-Å Mg/rubrene surface. Synchrotron-radiation photoelectron spectra showed that, following C_{60} deposition, Mg preferentially interacted with C_{60}. A strong energy shift of the vacuum level indicated the formation of an interfacial dipole layer caused by the negative charge transferred from Mg to C_{60}. A significant enhancement of the interfacial dipole potential and an increase in the separation between the highest occupied molecular orbital (HOMO) of rubrene and the lowest unoccupied molecular orbital (LUMO) of C_{60} revealed that the addition of Mg has a large possibility to improve ODD performance.

Synchrotron-radiation photoemission experiments were performed at the National Synchrotron Radiation Research Center (NSRRC), Taiwan. Photoelectrons were collected with a 125-mm hemispherical analyzer (OMICRON Vakuumphysik GmbH) in a UHV chamber. The total energy resolution was 100 meV for the valence-band spectra with a photon energy of 82 eV. All energies were calibrated with a gold mounted on the sample holder. The base pressure was less than 3.0×10^{-10} Torr, and the pressure was maintained at less than 3.0×10^{-9} Torr for all evaporations. An *n*-type, mirror-polished, Si(001) single crystal ($\rho = 1$–$10\ \Omega$ cm, P) was annealed in a stepwise manner to 1200 °C in the chamber to remove the protected oxide layers; this resulted in the surface appearing free from residual impurities. The rubrene sample was prepared by vacuum deposition of thoroughly degassed rubrene (99.99%, Sigma-Aldrich) from a Knudsen cell at 115 °C on a clean Si(001) surface. The thickness of the rubrene film was controlled at approximately 60 Å, which is sufficiently thin to avoid charging, and yet thick enough to suppress emissions from the silicon substrate. The Mg was deposited sequentially *in situ* from a Mo crucible, and then thoroughly degassed C_{60} was deposited from a boron nitride (BN) crucible onto the Mg/rubrene surface held at room temperature. The extent of coverage was determined using a quartz oscillator monitor, and a monolayer (ML) of C_{60} was estimated to be 10 Å thick (outer diameter).

The evolution of the Mg 2p core-level spectra of a 4-Å Mg/rubrene film with varying coverage of C_{60} molecules is shown in Fig. 1(a), where the photoelectron intensities are normalized by their individual background heights. All binding energies (BEs) are referenced relative to the Fermi level of Au, E_F. Each curve is denoted with the corresponding C_{60} thicknesses, as θ_{C60}, in units of ML. The spectrum corresponding to 0 ML is for the 4-Å Mg/rubrene film, which consists of one sharp component, P, at a BE of 49.56 eV, and a large broad component, P_R, at 51.22 eV BE. As shown in Fig. 1(b), by comparing this spectrum with that of a pure Mg film, we could identify that the peak P comes from the non-reacting Mg cluster. Peak P_R was therefore assigned to be the emission from Mg reacting with the rubrene. The BE of P_R is higher than that of the neutral component P by 1.66 eV, indicating that negative charges are transferred from Mg to the rubrene.

After C_{60} deposition, the broad peak shifted toward the lower BE, and P decreased concomitantly. With increasing

a)Author to whom correspondence should be addressed. Electronic mail: cpcheng@mail.ncyu.edu.tw

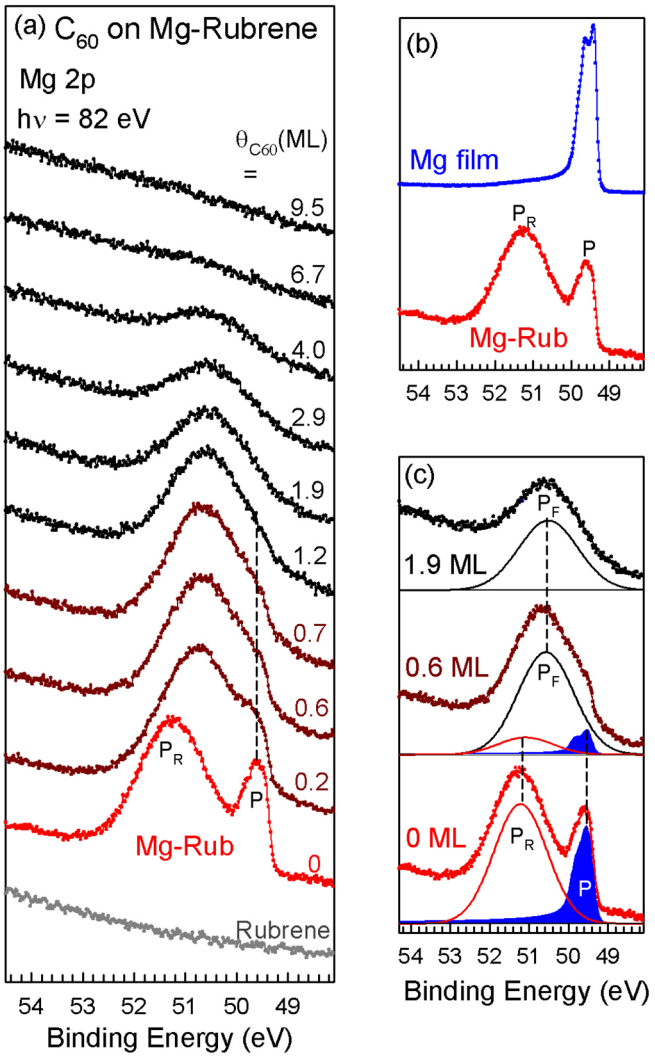

FIG. 1. Mg 2p core-level spectra recorded with a photon energy of 82 eV. (a) The evolution of the spectra for a 4-Å Mg/rubrene film with varying C_{60} coverage. (b) A comparison of the Mg 2p cores of a Mg/rubrene film with that of a pure Mg film. (c) Representative curve-fitting results of the Mg 2p cores.

C_{60} coverage, P diminished gradually until disappearing at $\theta_{C60} = 1.2$ ML. At 1.9 ML, only one broad peak was observed, and when the C_{60} coverage reached 6.7 ML, no Mg 2p signal was present. To learn more about the broad peak, we fit the Mg 2p spectra using a least squared fitting method with Voigt functions, and present representative results of 0 ML, 0.6 ML, and 1.9 ML in Fig. 1(c). A singularity index (Doniach-Ŝunjić line shape) of 0.13 was used for the Mg-cluster component P. To obtain a consistent position for each component in all coverage levels, a third component P_F had to be included in the model function at the sub-monolayer level. Therefore, the BEs obtained for P, P_F, and P_R are 49.55 ± 0.02, 50.57 ± 0.07, and 51.16 ± 0.06 eV, respectively. We observed a Lorentzian width of 0.028 ± 0.002 eV (full width at half maximum, FWHM), in good agreement with the 0.03 eV width obtained from a Mg film on a Si(001) surface.[8] The spin-orbit splitting and branching ratio are 0.29 ± 0.02 eV and 0.56 ± 0.04, respectively.

As Fig. 1(c) shows, C_{60} deposition generated a new component P_F and simultaneously degraded the components P and P_R. With increasing C_{60} coverage, the intensity of P_F increased, whereas those of P and P_R decreased. At 1.9 ML, only the P_F peak existed, suggesting that P_F originated from the Mg interacting with the C_{60}. The reduction of not only P but also P_R at the sub-monolayer level indicates that Mg is attracted to C_{60} more than to rubrene, one reason for which could be the higher electron affinity of C_{60} than of rubrene.[9–11] The P_F peak appeared on the higher-BE side of the P peak, which indicates that the Mg atoms that contribute to P_F must have more positive charges than those that contribute to the neutral component P. The negative charges lost by Mg can go nowhere but to C_{60}.

Valence-band spectra with the same coverage levels as in Fig. 1(a) are shown in Fig. 2. The right-hand panel in the figure shows a magnification of the spectra in the vicinity of E_F, and the left-hand panel presents the low-energy cutoff. Each curve is denoted with θ_{C60}, as well as with the change in the low-energy cutoff, ΔE_c, in eV. The bottommost curve, obtained with a thick rubrene film, reveals sharp molecular features that are in good agreement with previous photoemission results of rubrene films.[12–14] The H_R, A, and C peaks are characteristic of the tetracene-like backbone, whereas peak B and the remainder of the spectrum at a higher BE are dominated by the contributions from phenyl groups.[13]

As shown in Fig. 2, after the addition of Mg atoms, the spectrum clearly shifts to a higher BE, which results from the movement of E_F toward the LUMO-derived band of rubrene because of the transfer of negative charge from Mg to the rubrene. The H_R, A, and C are smeared, whereas the shapes of the other features resemble those in pure rubrene, indicating that the added Mg mostly adsorbs on the backbone and has little effect on the electronic structure of the phenyl groups.

The deposition of C_{60} on the Mg/rubrene film immediately reversed the spectrum movement toward a lower BE. This result indicates that the negative charges formerly transferred from the Mg to the rubrene reduce leading to the shift of E_F away from the LUMO of rubrene, consistent with the reduction of the component P_R in Figs. 1(a) and 1(c). With increasing C_{60} coverage, the C_{60}-derived features gradually replace the states originating from rubrene, and when the coverage reaches 4.0 ML, the spectrum is dominated by the C_{60}-related molecular orbital. At 9.5 ML, the HOMO of C_{60}, labeled H_F and located at a BE of approximately 2 eV, is typical for bulk fullerene.[15,16] At less than 9.5 ML coverage, the C_{60}-related features appear at higher BE than those in bulk fullerene, further confirming that C_{60} molecules contact Mg atoms with negative charges. Furthermore, the large ΔE_c across the C_{60}/Mg-rubrene heterointerface demonstrates the formation of an interfacial dipole layer due to the charge transfer.

To understand the effect of Mg addition on C_{60}/rubrene heterojunctions, we selected the 2.9-ML coverage of C_{60} to plot an interfacial energy-level diagram shown in Fig. 3(a). For comparison, in Fig. 3(b), we plot the energy-level diagram for the 2.9-ML C_{60}/rubrene interface without Mg. Both diagrams were derived from the photoemission data shown in Figs. 3(c) and 3(d), respectively. Because the energy-level alignment at organic/organic interface depends critically on the substrate,[17] the experiment of C_{60}/rubrene without Mg were also performed with Si(001) as substrate. The LUMO

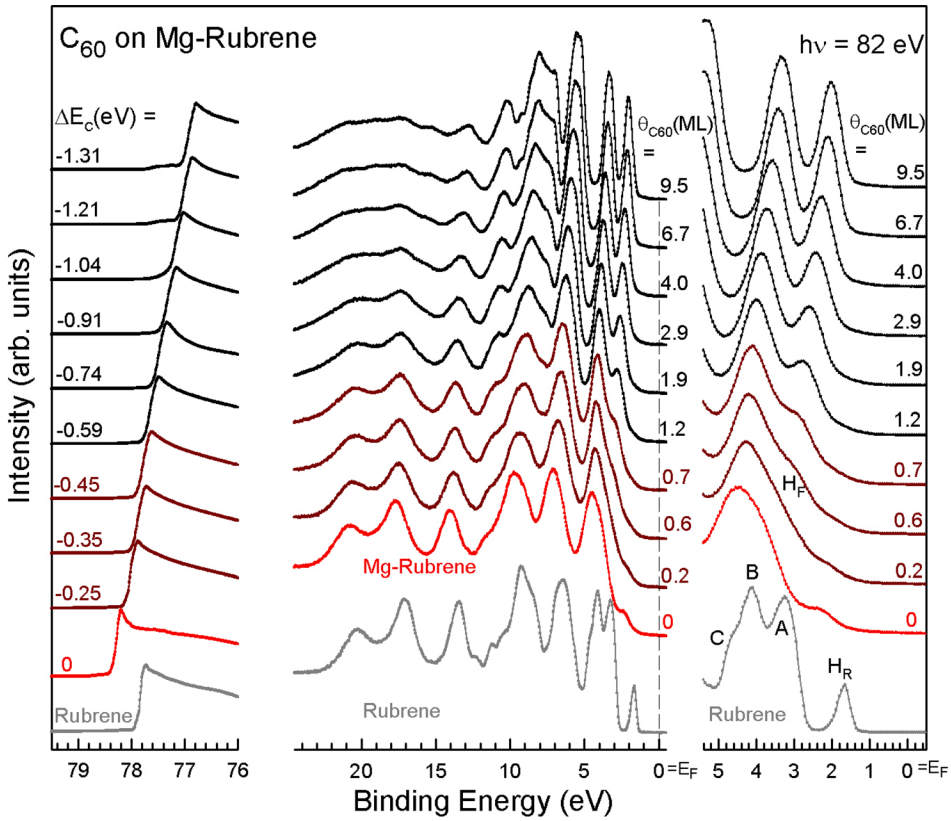

FIG. 2. Valence-band spectra recorded with a photon energy of 82 eV for C_{60} on a 4-Å Mg/rubrene surface. The right-hand panel shows a magnification of the spectra in the vicinity of the Fermi level, E_F. The left-hand panel is the low-energy cutoff. Each curve is denoted with the C_{60} thickness, θ_{C60}, in ML, as well as with the change in the low-energy cutoff, ΔE_c, in eV.

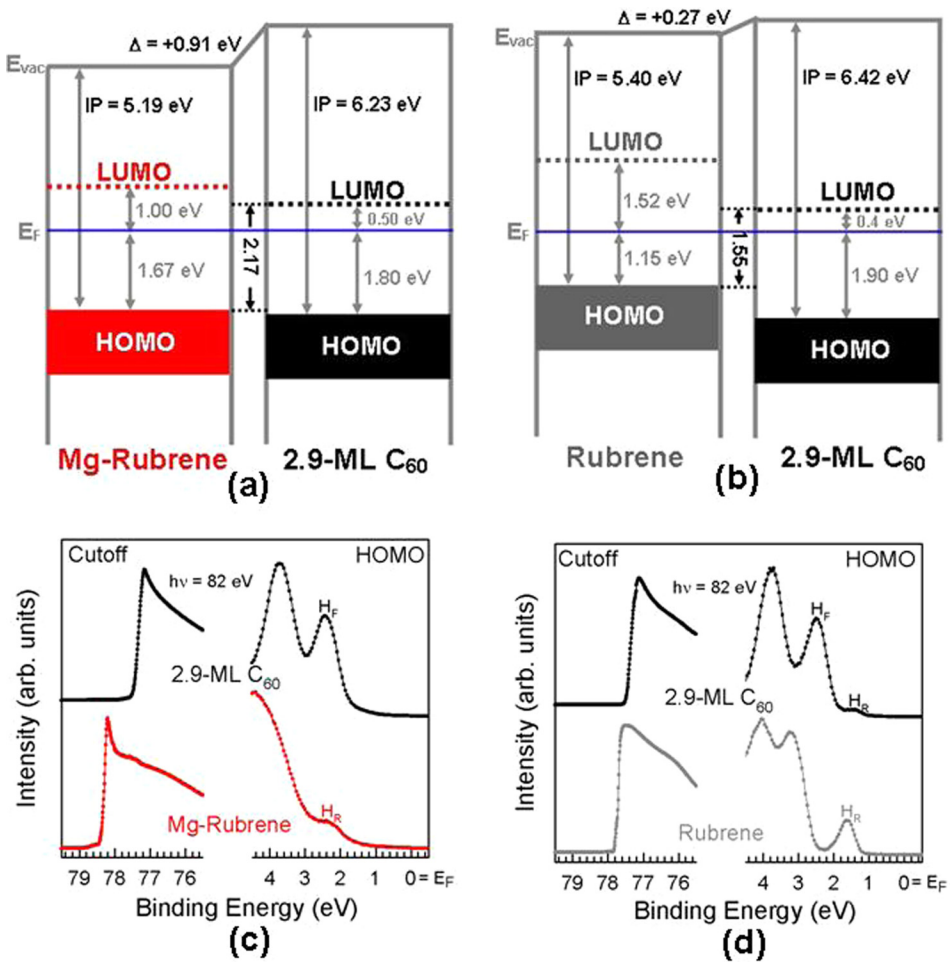

FIG. 3. The interfacial energy diagram for 2.9-ML C_{60}/rubrene heterojunctions, (a) with Mg, and (b) without Mg, derived from the corresponding photoemission data shown in (c) and (d).

energies of rubrene and C_{60} were determined from the energy gap to be approximately 2.67 and 2.3 eV,[18,19] respectively, and the energy differences were measured from the onset of the peak. The ionization potential (IP) of the film was determined using the equation $IP = h\nu - W$, where W is the energy difference between the onset of HOMO and the low-energy cutoff. The IPs of 5.40 and 6.42 eV for rubrene and C_{60}, respectively, in Fig. 3(b), agree with those of pristine materials.

The addition of Mg clearly induced critical changes at the C_{60}/rubrene. First, the IPs of both, rubrene and C_{60}, in Fig. 3(a) are smaller than in Fig. 3(b) by around 0.2 eV. The discrepancy in IP is attributed to the interaction with Mg. This finding further confirms that, following C_{60} deposition, the Mg atoms, original on the rubrene film, interact with C_{60}. Second, the interfacial dipole potential increases significantly, by nearly 0.64 eV, due to the charge transfer at the interface. The direction of the interfacial dipole pointing to the rubrene side is expected to decrease the built-in potential, V_{bi}. Because rubrene and C_{60} serve as the hole transport layer and electron transport layer, respectively, for the light-generation application, the increase of the dipole potential would favor a decrease in the electroluminescence turn-on voltage. Third, a marked increase of almost 0.62 eV was observed in the separation between the LUMO of C_{60} and the HOMO of rubrene. In an organic *p-n* junction, the optimum value of an open circuit voltage, V_{OC}, is generally expected to be the energy level difference between the LUMO of the acceptor and the HOMO of the donor.[20] Thus, the addition of Mg at the C_{60}/rubrene heterointerface has a high probability of increasing V_{OC} and thereby enhancing the efficiency of photovoltaic cells.

We further investigated the dependence of the expected optimum V_{OC}, denoted as V_{OC_OPT}, on the interfacial dipole potential. V_{OC_OPT} and the dipole potential are presented as functions of C_{60} coverage in Fig. 4. The separation of the LUMOs, ΔE_{LUMOs}, between rubrene and C_{60} was also plotted to examine the capacity of photoexcitons to dissociate. As shown in Fig. 4, with the addition of Mg, V_{OC_OPT} enhances by 0.28 eV at least. Variation in V_{OC_OPT} strongly correlates with changes in the interfacial dipole, increasing with the dipole potential, and both approach a saturation of above 6.7 ML. Thus, V_{OC_OPT} improves with an increase of the interfacial dipole moment, which can benefit the development of light- and current-generating ODDs.

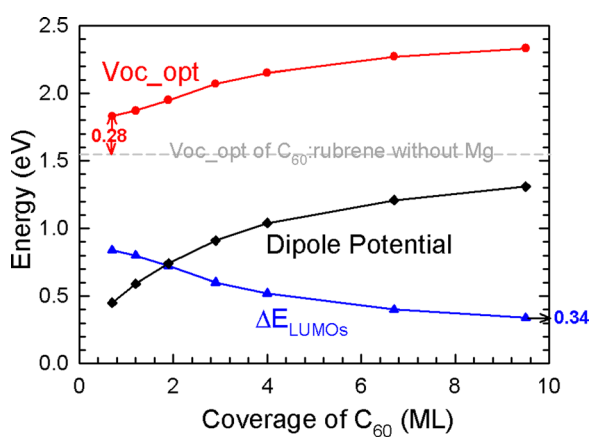

FIG. 4. The inverse relationships of V_{OC_OPT} and ΔE_{LUMOs} with the interfacial dipole potential.

The interfacial dipole raises C_{60} energy levels and enhances V_{OC_OPT} but also simultaneously reduces ΔE_{LUMOs}. The dissociation of photoexcitons at the donor/acceptor interface must be mediated by a drop in the LUMO potential between the donor and the acceptor, and ΔE_{LUMOs} with moderate values is required to prevent photoexcitons from recombining. As shown in Fig. 4, ΔE_{LUMOs} decrease with increasing dipole potential. After 6.7 ML, the variation becomes small. At 9.5 ML, a saturation value of almost 0.34 eV is attained for ΔE_{LUMOs}, a value that should be high enough to provide a barrier against photoexciton recombination.

In summary, we studied the interfacial electronic structure of C_{60} on a 4-Å Mg/rubrene surface. The photoelectron spectra showed that Mg prefers to interact with C_{60} than with rubrene. Negative charge transferred from Mg to C_{60} enhances the interfacial dipole potential, leading to an increase in the separation between the HOMO of rubrene and the LUMO of C_{60}. This modification of interfacial properties results in a decrease in V_{bi} and an increase in V_{OC_OPT}, demonstrating that the addition of Mg should be an effective method for improving the efficiency of light- and current-generating ODDs.

This project was sponsored by the National Science Council under the Contract No. 99-2112-M-415-009-MY3.

[1]H. Aziz and Z. D. Popovic, Appl. Phys. Lett. **80**, 2180 (2002).
[2]M. Y. Chan, S. L. Lai, M. K. Fung, C. S. Lee, and S. T. Lee, Appl. Phys. Lett. **90**, 023504 (2007).
[3]C. H. Chuen and Y. T. Tao, Appl. Phys. Lett. **81**, 4499 (2002).
[4]A. K. Pandey and J.-M. Nunzi, Adv. Mater. **19**, 3613 (2007).
[5]V. Podzorov, E. Menard, A. Borissov, V. Kiryukhin, J. A. Rogers, and M. E. Gershenson, Phys. Rev. Lett. **93**, 086602 (2004).
[6]C.-P. Cheng, W.-Y. Chen, C.-H. Wei, and T.-W. Pi, Appl. Phys. Lett. **94**, 203303 (2009).
[7]C.-F. Shih, K.-T. Hung, H.-J. Chen, C.-Y. Hsiao, K.-T. Huang, and S.-H. Chen, Appl. Phys. Lett. **98**, 113307 (2011).
[8]E. S. Cho, C. H. Lee, C. C. Hwang, J. C. Moon, J. h. Oh, K. Ono, M. Oshima, K. S. An, and C. Y. Park, Surf. Sci. **523**, 30 (2003).
[9]C. J. Brabec, N. S. Sariciftci, and J. C. Hummelen, Adv. Funct. Mater. **11**, 15 (2001).
[10]Y. Hamada, H. Kanno, T. Tsujioka, H. Takahashi, and T. Usuki, Appl. Phys. Lett. **75**, 1682 (1999).
[11]Z.-L. Zhang, X.-Y. Jiang, S.-H. Xu, T. Nagatomo, and O. Omoto, Synth. Met. **91**, 131 (1997).
[12]C.-P. Cheng, Y.-W. Chan, C.-F. Hsueh, and T.-W. Pi, J. Appl. Phys **112**, 023711 (2012).
[13]C.-P. Cheng, T. L. Li, C.-H. Kuo, and T.-W. Pi, Org. Electron. **14**, 942 (2013).
[14]L. Wang, S. Chen, L. Liu, D. Qi, X. Gao, and A. T. S. Wee, Appl. Phys. Lett. **90**, 132121 (2007).
[15]C.-P. Cheng, T.-W. Pi, C.-P. Ouyang, and J.-F. Wen, J. Vac. Sci. Technol. B **23**, 1018 (2005).
[16]J. H. Weaver, J. L. Martins, T. Komeda, Y. Chen, T. R. Ohno, G. H. Kroll, N. Troullier, R. E. Haufler, and R. E. Smalley, Phys. Rev. Lett. **66**, 1741 (1991).
[17]W. Chen, D.-C. Qi, H. Huang, X. Gao, and A. T. S. Wee, Adv. Funct. Mater. **21**, 410 (2011).
[18]H. Ding and Y. Gao, Appl. Phys. A **95**, 89 (2009).
[19]R. W. Lof, M. A. van Veenendaal, B. Koopmans, H. T. Jonkman, and G. A. Sawatzky, Phys. Rev. Lett. **68**, 3924 (1992).
[20]P. Peumans, A. Yakimov, and S. R. Forrest, J. Appl. Phys **93**, 3693 (2003).